The effect of anaerobic influent contact regime on granulation

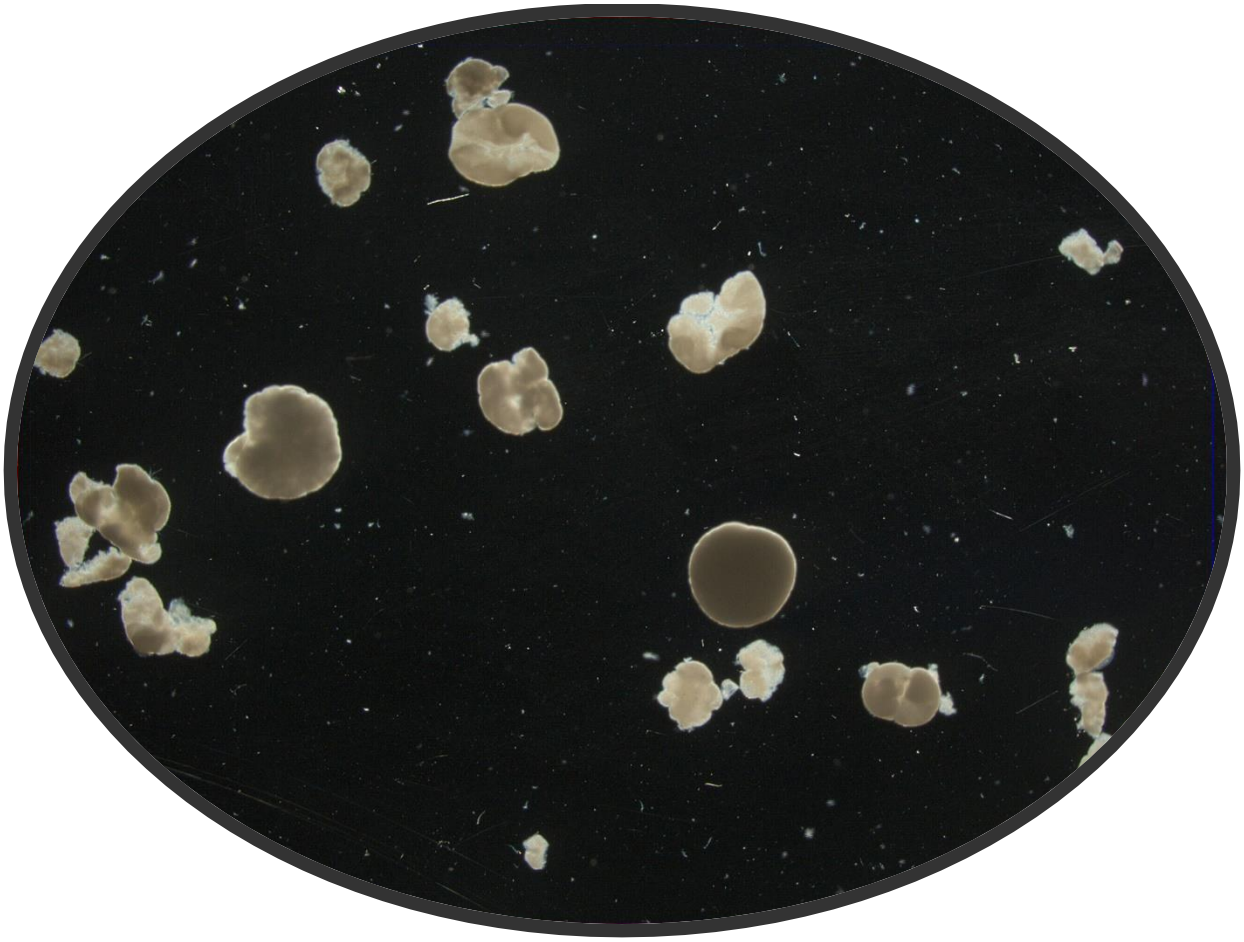

Granule distribution and characterisation of Aerobic Granular Sludge

Madelon Schouteren
10 October 2019
TU Delft

The effect of anaerobic influent contact regime on granulation

Granule distribution and characterisation of Aerobic Granular Sludge

Madelon Schouteren

In partial fulfilment of the requirements for the degree of

Master of Science in Life Science and Technology

at the Delft University of Technology

Supervision:

Ir. V.A. Haaksman	TU Delft, Faculty of Applied Sciences
Dr. ing. M. Pronk	TU Delft, Faculty of Applied Sciences

Thesis committee:

Prof. dr. ir. M.C.M. van Loosdrecht	TU Delft, Faculty of Applied Sciences
Dr. ing. M. Pronk	TU Delft, Faculty of Applied Sciences
Dr. ir. A. Wahl	TU Delft, Faculty of Applied Sciences

Abstract

Nowadays the use of aerobic granular sludge, also known as Nereda™ in municipal wastewater treatment, is applied worldwide. The next innovation in for this technology is the implementation of granular sludge in continuous flow through configuration. However, many challenges will have to be faced before this technology can be applied in full scale wastewater treatment plants. One of these is the formation and behaviour of granular sludge in continuous flow reactors. In this study the start-up and steady state behaviour of two lab-scale bioreactors were compared on growth speed, granule size distribution, influent distribution and density.

One of the reactors was run with an up flow feeding through the sludge bed, as performed in Nereda™ plants. The second reactor was run with a pulse feeding, followed by an anaerobic mixing phase. By combining data from image analysis with reactor cycle measurements, batch tests, PHA determination and density measurements, a classification of the granule size distribution and COD distribution over the granules was made. A comparison between the reactors could be made, as both reactors were exposed to the same conditions, except for their anaerobic influent regime.

Both reactors were fully granulated at the end of reactor operations. The bed fed reactor had a faster average growth speed of granules due to the higher COD load on the biggest granule fraction. This selected for a higher mass fraction of granules greater than 1mm in diameter in the bed fed reactor. Both reactors seemed to suffer from diffusion limitation, as oxygen limitation was observed in the bed fed reactor, while the pulse fed reactor showed spatial COD limitation. Both reactors experienced some degree of P-limitation.

The results from this study can be used to model granulation and granule metabolism of aerobic granular sludge exposed to different anaerobic contact regimes.

Contents

1. Introduction

The greatest recent innovation in municipal wastewater treatment is the use of Aerobic Granular Sludge (AGS)(Pronk *et al.*, 2015), also known as the Nereda™ technology. Improvements of AGS compared to traditional activated sludge (AS) is the improved settleablity of the granules, resulting in a smaller surface area of the wastewater treatment plants (WWTP). Moreover, due to substrate concentration gradients the layered granules, processes as simultaneous nitrification and denitrification (SND) can be utilised, (Mosquera-Corral *et al.*, 2005).

The AGS technology is currently applied in sequencing batch reactors (SBR). In a SBR selective pressure on settling speed and the 'Race to the Bottom' is used to push granular growth (Pronk *et al.*, 2015). The combination of these techniques removes sludge with bad settling characteristics, and favours the fastest settling granules by feeding influent, and thus COD via the bottom of the reactor.

In order to utilise this technology in full scale wastewater treatment plants (WWTP), new installations have to be built as SBR. However, most current WWTP are built in continuous flow-through configuration, meaning that conversion of these WWTPs to AGS technology is not always feasible. Therefore, recent developments in AGS are focussed towards using AGS in continuous processes (Kent *et al.*, 2018).

The mechanisms to grow aerobic granules can be divided in two main factors; growth and decay. Growth of granules is dependent on the COD load of a sludge particle and the solids retention time (SRT) of that particle. The decay of the granules is the sum of many factors, including; selective pressure on settling velocity, detachment, and the SRT limit. As long as the product of the COD load and the SRT is bigger than the sum of the decay, granule formation and growth is possible.

As a granule needs to be a certain size to sink through the sludge blanket, selection based on granule size is hard in the start-up of AGS reactors. The initial granules are not yet big enough to sink through the flocs, to prevent washout at high selective settling pressure. This pressure is one of the defining factors for granule growth, but it cannot be used during the start-up. Selective settling pressure was introduced in bioP continuous systems, however no granulation was found at a rate comparable to the granulation in a Nereda™. Therefore, granular growth is leading in achieving the minimal granule size to sink through the sludge blanket.

Phosphate accumulating organisms (PAO) have been shown to be the most dominant in granule growth and formation (De Kreuk and Van Loosdrecht, 2004). The slow growth of the PAO on storage polymers favours denser biofilm growth; granules (Picioreanu *et al.*, 1999). The use of a feast/famine regime with anaerobic storage would be most optimal to grow aerobic granular sludge (De Kreuk and Van Loosdrecht, 2004).

There are several methods of anaerobic influent contact used in continuous flow WWTPs. Influent can be added to a continuous stirred tank reactor (CSTR), or under plug flow conditions. With plug flow conditions a distinction can be made in the usage of a selector, upflow or normal plug flow conditions. In a selector a part of the sludge return flow is brought into contact with the influent, reducing dilution of the influent by mixing with water from the return flow. An upflow is typically used in Nereda™, where the influent is fed from the bottom of a sequencing batch reactor (SBR), without any influent dilution. Under normal plug flow condition the whole sludge return flow is mixed with the influent, resulting in a 1:1 dilution. Anaerobic influent contact using a selector(Amanatidou *et al.*, 2016) and plug flow(Jafarinejad, 2017), are proven to reduce filamentous growth in full scale WWTPs.

The different methods of influent contact are experienced differently by the sludge. When we view the anaerobic contact time from the point of a granule, a differences between the methods can be characterised. Assuming that a granule travels through a WWTP, it will move though the different compartments and experiencing different conditions, where every pass though the settler starts a new 'cycle' for the granule. This cycle can be divided in 3 steps, influent phase, aerobic phase, and settling phase.

In Figure 1 the different ways of anaerobic influent contact are compared on three characteristics: max COD influent concentration, change in COD concentration over the influent phase, and probability distribution over multiple cycles.

In a CSTR, the influent is added to a mixed tank, meaning that the maximal COD concentration is low (=effluent concentration), the change in COD concentration over the anaerobic time is low. However the change in COD load per cycle differs, as the residence time in the reactor changes per cycle.

For the Bed Feed method, as used in Nereda™, the bottom granules see the same high COD concentration (influent concentration), for the whole influent phase. This is the same for every new cycle, provided that in the settling phase stratification occurs. Without stratification, the place in the sludge bed is different for each cycle, resulting in a distribution in sludge load per cycle.

A perfect plug flow would have a medium COD concentration at the start, as the influent is diluted by the return sludge flow. As the COD is consumed, the COD concentration will decrease over the anaerobic time. As all the sludge is in the return flow, the COD load is equal for every cycle.

Using a selector, part of the sludge is brought into contact with the influent, leading to a medium to high max COD concentration, due to some dilution of the sludge return flow. The COD concentration decreases over the anaerobic time, leading to a high change in COD concentration. As only part of the sludge is brought into contact with the COD, the dispersion in COD load per cycle is high.

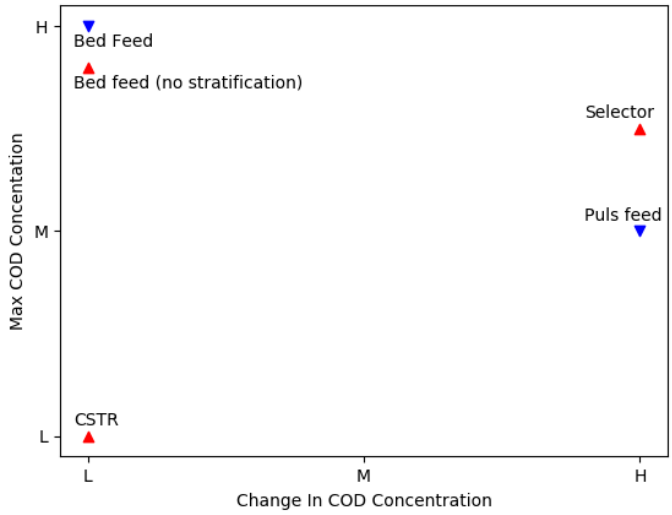

Figure 1: Influent regime graph with (▲) indicating a high difference in sludge load per cycle, and (▼) indicating a narrow distribution in load per cycle, the Bed Feed without stratification should be in the same spot as the Bed Feed, but shown slightly lower for visibility

In this study we followed the start-up process of AGS systems with two different anaerobic contact regimes. One reactor being a Nereda™-like SBR, this reactor was slowly fed with influent from the bottom of the reactor, resulting in a plug flow thought the bed. When stratification occurs in the bed, the fastest settling sludge receives a higher COD load, than sludge at the top of the sludge bed. The second reactor had an anaerobic contact time that approached a plug flow regime. The plug flow was approached by applying a fast influent phase, followed by an anaerobically mixed phase. Resulting in an equal concentration gradient for every sludge particle. This reactor setup given the name pulse fed reactor, as the influent is pulsed into the reactor. The reactors both had the same setup, the only difference being the anaerobic influent contact method. Selective wasting was used to force the sludge towards fast settling and favouring the growth toward granulation. After the start-up phase, both reactors were given a SRT limit. Using the pulse fed reactor, the added benefit of settling speed for a higher COD load is removed. The growth of the granules was followed during the start-up to visualise the granule growth at different anaerobic contact regimes.

1.1 Research Questions

The results of this study can answer the following research questions: these are important to be able to help further research towards continuous AGS.

- What is the average growth speed of a granule during reactor start-up?
    - Does this differ with the anaerobic contact regime?
    - Does the growth speed of granules change with the granule size?
- Does the granule size distribution and growth differ during steady state with the anaerobic contact regime?
- Is there a relation between granule size and anaerobic rates?
    - Does this differ with the anaerobic contact regime?
    - How do these rates compare with full-scale granule rates?
- Is there a relation between granule size and anaerobic stoichiometry
    - Does this differ with the anaerobic contact regime?
    - How do these rates compare with full-scale granule rates?
- Does the biomass density differ with the anaerobic contact regime?
    - Is the density change with the granule size?
    - Is the density comparable with the full-scale granules?

During stable reactor operations, the different granule sizes were characterised on COD uptake rates, COD capacity, phosphate release rate, biomass density and COD distribution over the granules. The spread of granule sizes over both reactors was compared. Most of these test were also performed on granules from WWTP Utrecht where the water is treated with the Nereda™ technology. With this data the trend in anaerobic rates and storage capacity with respect to the granule size could be compared to full-scale granules.

2. Materials & Methods

2.1. Experimental set-up and operational conditions

Two double walled sequencing batch reactors with an internal diameter of 5.6 cm, 150 cm height and 3L of working volume were operated for 20 weeks under alternating anaerobic and aerobic conditions. The pulse fed reactor was equipped with nitrogen gas for anaerobic mixing during the anaerobic reaction phase.
The bed fed reactor was fed with influent after the settle and discharge phase, with a superficial velocity of 0.5 m/h through the sludge bed.
Before the start of the feeding, the pulse fed reactor was flushed with N_2 gas (5L/min) for 5 minutes, to remove residual oxygen of the aeration phase from the water. After flushing, the influent was added to the reactor within 2 minutes. This phase was followed by 1 hour of anaerobic mixing with nitrogen gas (5L/min), while controlling the pH at 7±0.1 by dosage of a 1M hydrochloric acid solution. After the anaerobic phase, the aerobic phase, with a length of 2 hours was started. During aeration, the offgas was recycled to keep a constant flow of 6L/min. Separate mass flow controllers for nitrogen gas and compressed air were used to ensure a dissolved oxygen concentration of 20±1%, at a temperature of 20˚C. The pH during aeration was 7±0.1 controlled by dosage of 1M hydrochloric acid and 1M sodium hydroxide solution. After aeration a settling phase of 3 minutes, imposing an 11.4 m/h settling velocity, was used to separate the sludge from the water. All sludge unable to meet the settling velocity, was washed out with the effluent.

The influent composition is shown in Table 1, a COD/P ratio of 40 and COD/N ratio of 20 was used. ATU was added to the influent to prevent nitrification in the reactor.

Table 1: Influent composition

Component	Concentration	Unit
COD (Acetate)	300	mg/L
MgSO4	0.072	mg/L
KCl	0.029	mg/L
NH4-N	15	mg/L
PO4-P	7.5	mg/L
ATU	0.005	mg/L
Vishniac's trace elements	0.118	mL/L

After the start-up, both reactors were kept at an average SRT of 20 days, by manually removing sludge from the reactor at the end of the aeration phase twice a week. The COD load of the reactor was 0.98 gCOD/L/d, divided over 7 cycles per day. During the cycles, electrolytic conductivity, redox, DO, pH and temperature were measured online.

2.1.1. Sampling procedures

All samples were taken via the sample ports at the side of the reactor, during anaerobic or aerobic mixing. Samples for image analysis, SRT control, density, and dry solids measurements were always taken at the end of the aeration phase. At the end of the reactor operations, the content of the reactor was collected in a bucket. The last sample for image analysis was taken from this bucket, to prevent sampling errors via the sample port.

From WWTP Utrecht granules were harvested at the start of aeration, these granules were aerated for two hours before the batch tests and density measurements were performed.

2.2. Start-up conditions

Both reactors were seeded with crushed granules from a stable, granulated SBR. The seed sludge particles had a diameter between 63 and 106 um, obtained by sieving the crushed granules. During start-up, the selective settling pressure was stepwise increased starting at 1.1 m/h to 11.4 m/h in 21 days. During the start-up, the only sludge removal was from the effluent withdrawal phase.

2.3. Granule development

The shifts of biomass between the fractions can be approached by combining the growth of a faction per day, with the amount of sludge leaving the fraction by selective wasting and the manual SRT control. In Figure 2 a simplification of the mass balance is shown. The COD from the influent was divided over the different fractions, leading to growth in the fractions. The fractions themselves contain a certain amount of sludge, this biomass distribution was determined by image analysis data. Sludge is removed from the reactor via selective wasting and manual SRT control, in Figure 2 this is shown by the black arrow leaving the fractions. The green arrow leaving the fractions indicates the net flow of the biomass in the fractions. This flow can leave the fraction, when the biomass growth in the fraction is higher than the biomass removal, and biomass leaves the fraction by growth or decay. When the flow enters the fraction, the biomass removal is higher than the growth of the fraction, and biomass is added to the fraction form growth of smaller fractions, or by decay from bigger fractions.
The calculation of each of these flows is explained in the following chapters. The granules were counted using image analysis and were divided over size fractions, corresponding to the used sieves to separate sludge for the batch tests. The particles were classified in the following fractions: <212, 212-400, 400-800, 800-1000, 1000-1400, >1400.

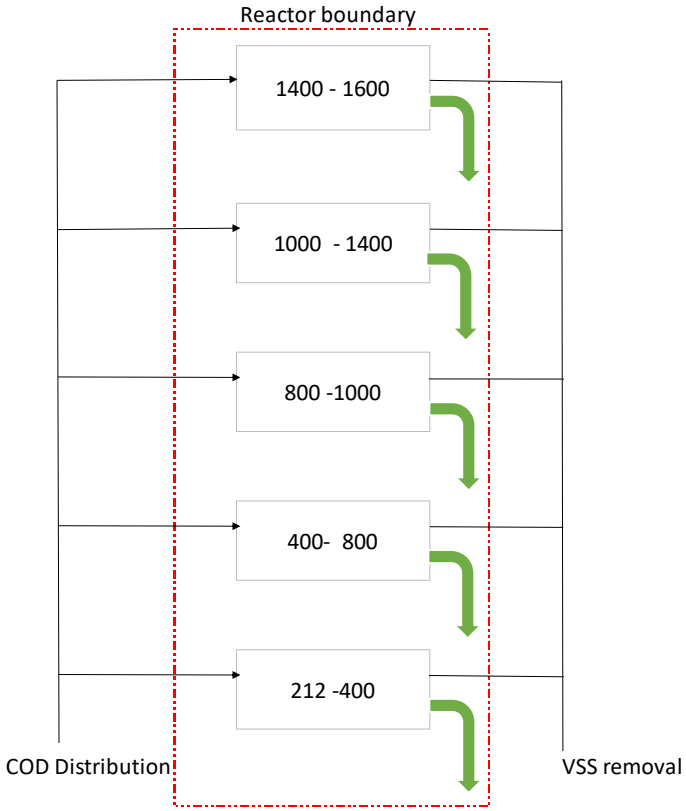

Figure 2: Massbalance of granulefractions in the labreactor

2.3.1. COD distribution

To determine the distribution of the available COD over the granule fractions, the PHB and PHV values of the granule fractions after the anaerobic reaction time were compared to the values at the end of aeration. The difference determined the change in gCOD/gVSS per cycle per fraction. The load per fraction is calculated by combining the change in gCOD/gVSS per fraction and the amount of sludge of that fraction in the reactor. From there the percentages of the influent COD are calculated and can be added to the left side of Figure 2. By combining the COD per fraction with the average yield, growth of each fractions was calculated.

2.3.2. Effluent distribution

The granules leaving the fraction were determined by combining the data of the selective wasting and the manual SRT control. Image analysis was used to determine the granule fractions in the effluent of the reactor. The area of the particles was used state the volume of the leaving particles, by assuming a perfect sphere for each granule. Together with the density, the weight percentage of that fraction in the effluent was calculated. The effluent and the SRT control determine the flow of each fraction out of the reactor, the black arrow leaving the fraction in Figure 2.

By setting up a mass balance over every fraction, the biomass shifts over the fractions were calculated. In the balance, a dynamic steady state is assumed, meaning that biomass can shift between the fractions while the biomass content of a fraction stays the same.

$$\frac{dM_i}{dC} = COD * F * f_{influent\ (i)} * Y - F * VSS_e * f_{i,e} - VSS_r * V * f_{i,r}\ /SRT/N - r = 0$$

In the balance COD is the COD concentration in the influent, F is the flow of influent (and effluent) per cycle, $f_{influent,(i)}$ is the fraction influent COD for the granule fraction. Y is the biomass yield of the reactor, VSS_e is the concentration VSS in the reactor effluent, $f_{i,e}$ is the granule distribution in the effluent. VSS_r is the concentration VSS in the reactor. V is the reactor volume. $f_{i,r}$ is the granule distribution in the reactor. SRT_i is the average sludge retention time in the reactor of that fraction. N is the number of cycles per day. r is the biomass flux leaving the granule fraction.

2.4. Batch test

To determine the specific acetate uptake rate and capacity, and the PO_4 release rate and capacity of the different granule fractions, batch tests were performed on the sludge fractions.

After 140 days, at the end of the aeration phase, sludge was withdrawn from the reactor and sieved over sieves (212, 400, 800, 1000, 1400 and 1600 um diameter) to split the sludge in five fractions. These sludge fractions were tested in an anaerobic batch setup. The sludge was added to filtered reactor effluent (63µm) buffered with a 0.1M HEPES buffer. The pH was set on 7±0.05 at the start of the batch test, the pH at the end of the test was 7.2±0.1. After 5 minutes of mixing with nitrogen gas (1±0.05 L/min) a first sample was taken for the initial PO_4-P concentration.
To start the test, COD was injected to an initial concentration of 500±100 mg/l to prevent any bias from diffusion limitation, as at this concentration even big granules should be fully penetrated with acetate within several minutes. For 30 minutes, every 5 minutes a sample was taken to determine the initial rate of PO_4-P release and acetate uptake. After 100, 105 and 110 minutes a sample was taken to determine total PO_4 release and acetate uptake. At the end of the test, a sample was taken to be analysed on granule size and morphology through image analysis. The final volume was calculated and residual biomass weight was measured. For result processing the biomass amount at every sample moment was calculated using the sample sizes and assuming biomass taken out through sampling had the same concentration as the reaction flask.

2.5. Analytical methods

Several analytical methods were used to determine the granule characteristics. The used analytical methods are explained below.

2.5.1. Biomass concentration

The biomass concentration in the reactor was measured in two ways; During steady state operations, the biomass in the reactor was determined by measuring the bed volume of the sample, and weighing the dry weight (after 24 h, on 105 C) and weighing the ash (after 2h, 550 C). With this information and the sludge bed volume in the reactor, the total TSS and VSS of the reactor were calculated.

During the start-up phase a mixed liquor method was used, as there was not yet a reliable sludge bed to refer to. In this method, a sample with a known volume was taken from the reactor, by weighing the dry weight and ash weight of this sample, the biomass concentration in the reactor was calculated.

2.5.2. Cycle measurement

The reactor conversions were measured weekly by sampling during the anaerobic reaction phase (pulse fed reactor only) and the aeration phase. The samples were immediately filtered over a 0.2 µm filter (Whatman FP30/0.2 CA-S) to remove all biomass. The samples were measured for PO4-P, NH4-N concentrations by photometric tests using a Gallery™ Discrete Analyzer. Acetate concentrations were measured by using HPLC, using an apolar column, a runtime of 30 minutes, and an injection volume of 20µL. The data from the samples was linked to the online measurements.

2.5.3. PHA content

PHA samples were taken after the anaerobic reaction time and at the end of the aeration time to determine the acetate uptake. The bed fed reactor was modified to accommodate anaerobic sampling after the feeding. During the feeding, the water above the sludge bed was stripped with nitrogen gas to remove residual oxygen, without disturbing the influent flow through the bed. After the feeding, nitrogen gas was used to mix the reactor to be able to take a representative anaerobic sample. The samples were inactivated with formaldehyde and subsequently sieved to be able to determine the PHB and PHV content of five different granule sizes. (212, 400, 800, 1000, 1400 and 1600 um diameter sieves used). The PHA content of the biomass was measured using the method of (Johnson *et al.*, 2009)

2.5.4. Biomass density

The absolute biomass density of the granules was measured using the Dextran Blue method (Beun *et al.*, 2002). A sieved fraction (212, 400, 800, 1000, 1400 and 1600 um diameter) of granules was put into a measuring cylinder, a known amount of dextran blue was added and the total volume and sludge volume (after 5 min settling) was measured. By comparing the absorbance of the water fraction to a reference absorbance line, the concentration of DB in the cylinder was calculated. Using this, the water fraction in the sludge bed could be calculated. By measuring the dry weight and VSS of the used sludge, the VSS mass per volume of granule was calculated. The absolute density shows how compact the granules grow.

2.5.5. Image Analysis

The growth of the granules was followed using Image Analysis (IA). During the start-up and the reactor operations, biomass samples were analysed on granule size using stereozoom microscopy. Each particle in a known volume was counted and characterised. As this is a 2D measurement and the biomass has a 3D shape, an uncertainty in the data has to be taken into account. To prevent background noise in the measurement, only particles with an area bigger than 4025 um^2 were accepted (a diameter of 36 um). Using the area, the equivalent diameter of a particle was calculated, assuming the particle is a circle. This diameter was further used to calculate the volume of the granules, assuming a spherical shape for every particle. Using this measurement, the volume and size of granules are roughly estimated, as a 3D shape is first characterised as a 2D shape, and then processed to characterise as a 3D shape. When taking into account that the found granules are not perfect spheres, some deviation between measurements is expected. Particles were identified based on their whiteness against a black background, as the granules have a light colour.

3. Results

3.1. Reactor start-up and granular growth

During the start-up it was not possible to achieve a plug flow influent regime in the bed fed reactor. As the reactors were seeded with crushed granules which formed a tightly packed sludge bed during the settling phase. The influent was not able to penetrate the sludge bed, resulting in a floating sludge bed and the formation of preferential flow channels though the bed. The floating sludge bed and the formation of the preferential flow channels can be seen in Figure 3. The absence of the plug flow regime though the bed led to available COD in the aeration phase, fuelling fast aerobic growth. This growth led to flocculent biomass formation attached to the growing granules. The resulting flocs had a higher settling velocity than the used selective settling pressure. After three weeks, the flocculent growth disappeared quickly when the anaerobic capacity of the sludge was high enough to remove all COD anaerobically. The difference between the flocculent sludge and a fully granulated reactor can be seen in Figure 3.

The pulse fed reactor had no start-up issues, as within a week all COD was taken up anaerobically, before aerobic growth was able to result in big sludge flocs. However, a high sludge concentration was noticed during the start of the effluent phase at every cycle. It was found that during the flush and mixing phases, some granules were deposited in the effluent discharge tube of the pulse reactor.

The start-up of a bed fed reactor is challenging, as the plug flow in the reactor relies solely on the stability of a granulated sludge bed, which is not present during start-up.

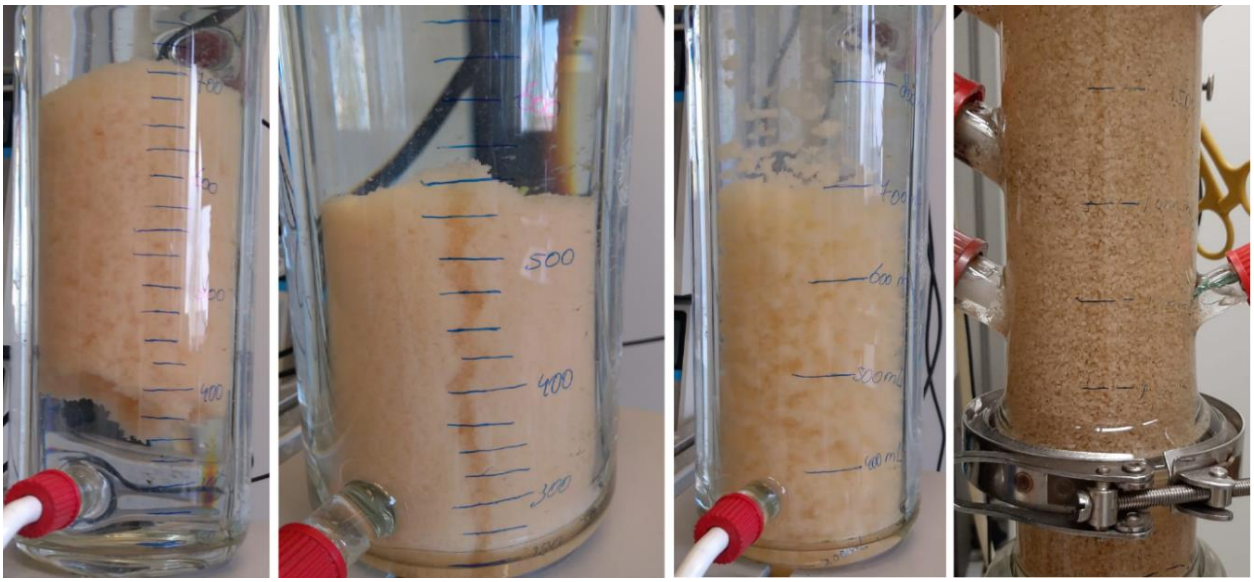

Figure 3: Picture 1 floating sludge bed during influent feeding. Picture 2: Preferential flow canals in the sludge bed during feeding. Picture 3: flocculent growth led to big sludge flocs. Picture 4: Fully granulated reactor.

The granule growth and distribution were followed over the course of the reactor operations (20weeks). The change in granule size distribution in both reactors can be seen in Figure 5. With this data the growth of granules during the reactor operation was meant to be followed. However, during the start-up fast flocculent aerobic growth and granules sticking to each other prevent reliable granule characterisation, pictures from the image analysis are shown in Figure 4.

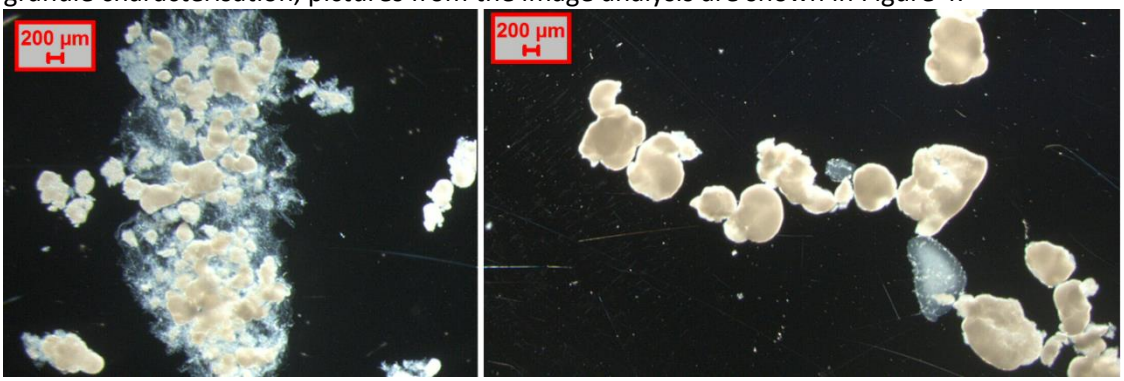

Figure 4: Flocculent growth connected sludge granules (left). Granules sicking to other granules during image analysis (right)

After the start-up difficulties, lasting for 3 weeks, granulation in the reactors was established. The trends in Figure 5 seem unstable for the granule fractions above 1mm diameter. To exclude sampling errors via the sampling port, the analysis of day 140 was performed on a sample taken from the reactor sludge mixed in a bucket. The results of this sample were compared to the most recent image analysis results of that reactor. The granule distribution of both samples can be seen in Figure 6. The difference in abundance of the 1400 µm fraction indicates towards an underestimation of this granule fraction. This could be caused by insufficient aerobic mixing during the reactor operations. Therefore the distribution of granules over the reactor operations is not reliable, but can be used indicative to determine when the first granules of a certain size are present in the reactor. The granule distribution on day 140 is deemed reliable to represent the reactors, due to the different sample procedure.

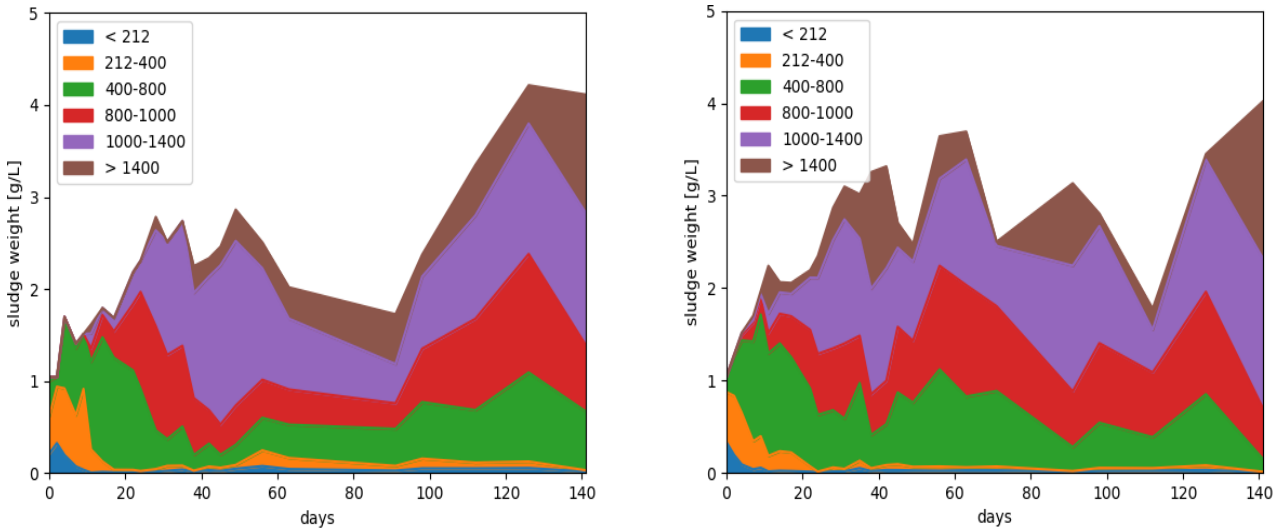

Figure 5: Granule growth distibution of the pulse fed reactor (left) and bed fed reactor (right) during the reactor operations

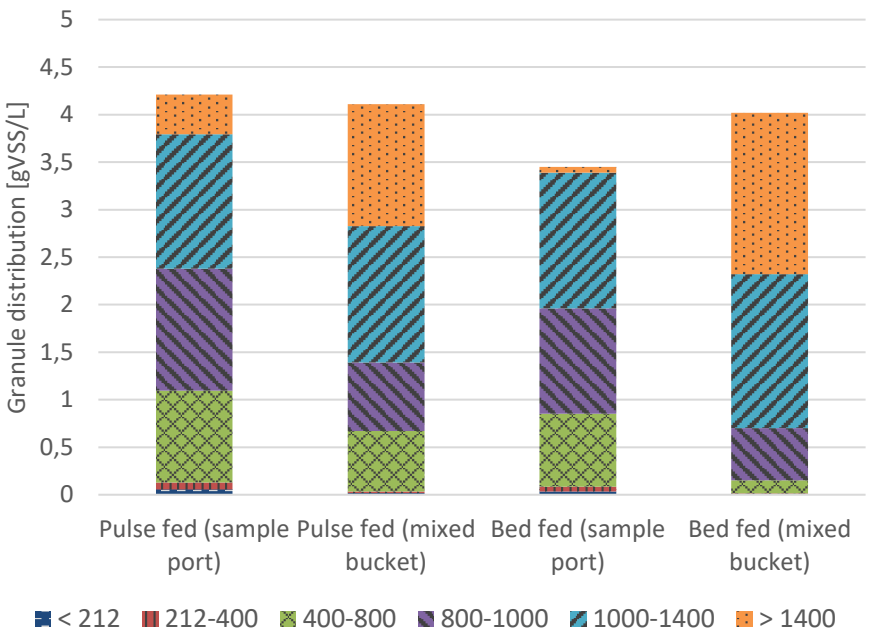

Figure 6: Granule distribution comparison with different sampling methods

In Figure 7 the first significant occurrences (>10w%) of each granule fraction in the pulse fed and bed fed reactor are shown. The influent contact regime of the bed fed reactor led to a higher COD load of the biggest granule fraction. This made the bed fed reactor reach a granule size of more than 1400µm faster than the pulse fed reactor. The COD distribution led to a higher average growth speed of 40µm/day, compared to a growth speed of 26µm/day in the pulse fed reactor.

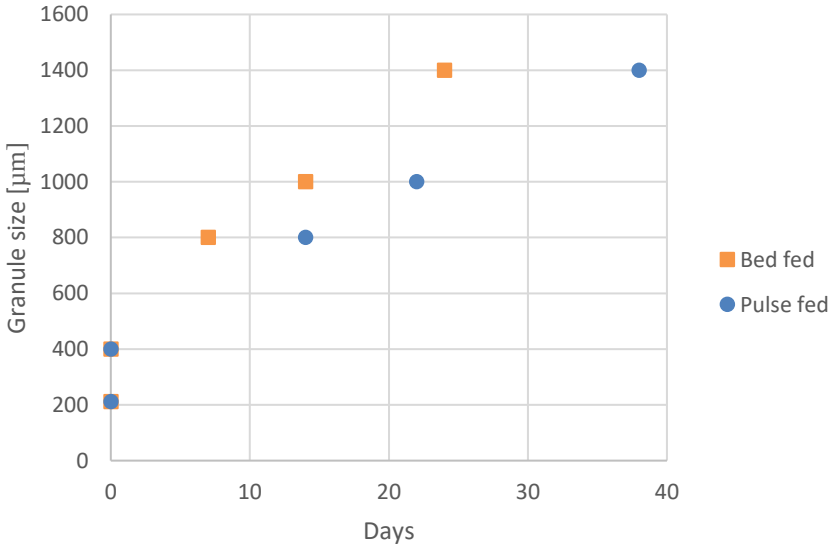

Figure 7: First occurance of granule sizes in the pulse fed and bed fed reactor

3.2. Cycle measurements

The average reactor rates can be obtained from the cycle measurements on the lab reactors. As both reactors have a similar VSS content, reactor rates are easy to compare based on the cycle data. In Figure 8 a cycle of the pulse reactor is shown. At t=0 the cycle starts with the influent phase, followed by the anaerobic reaction phase until t=65. After the anaerobic phase, the aeration is started until t=200, after which a new cycle starts.

Figure 8 shows the online measured pH and conductivity and the offline measured NH_4-N, PO_4-P and acetate concentrations during. Via the conductivity the phosphate release and uptake can be tracked. Phosphate release is seen during the anaerobic phase, however the phosphate release seems to continue after acetate is depleted. The increase in PO_4-P concentration between t=45 and t=60 can be explained by endogenous phosphate release. However it is unclear if the increase between t=15 and t=30 is originating from biological activity or diffusion from the granules.

At the end of the aeration the conductivity value keeps rising due to the pH control in the reactor. The decrease of the NH_4-N concentration shows the growth of the sludge during the aeration phase. At the end of the aeration the growth has stopped, as can be seen by the unchanging NH_4-N concentration.

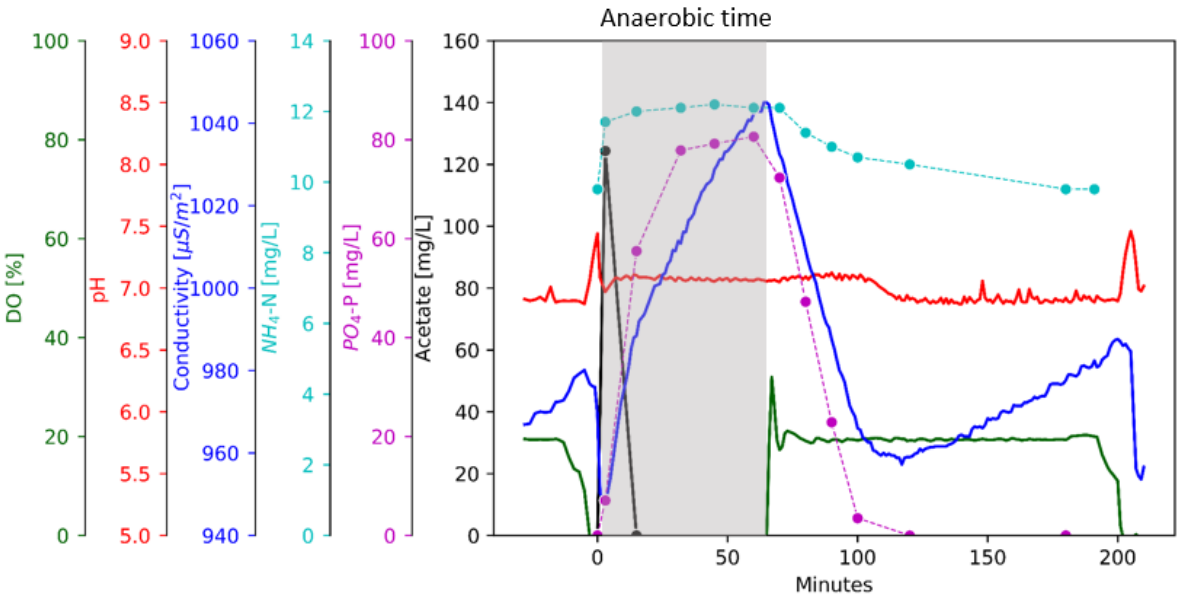

Figure 8: Representation of the dynamics in the pulse fed reactor during a cycle

In Figure 9 a cycle of the bed fed reactor is shown. It was not possible to sample during the anaerobic phase, due to the plug flow feeding through the bed. The online measurements are also not representative due to the lack of mixing. It is however possible to see when the influent reaches the pH sensor, as a dip in pH is seen. In the aeration phase, phosphate uptake and growth take place in the reactor. The PO_4-P concentration shows less phosphate release in the bed fed reactor compared to the pulse fed reactor. Both the phosphate release and the phosphate uptake rate are 2 times lower in the bed fed reactor. In the bed fed reactor a constant decrease in NH_4-N concentration can be seen during the aerobic phase. This indicates residual storage polymers in the sludge as there is still growth at the end of the cycle.

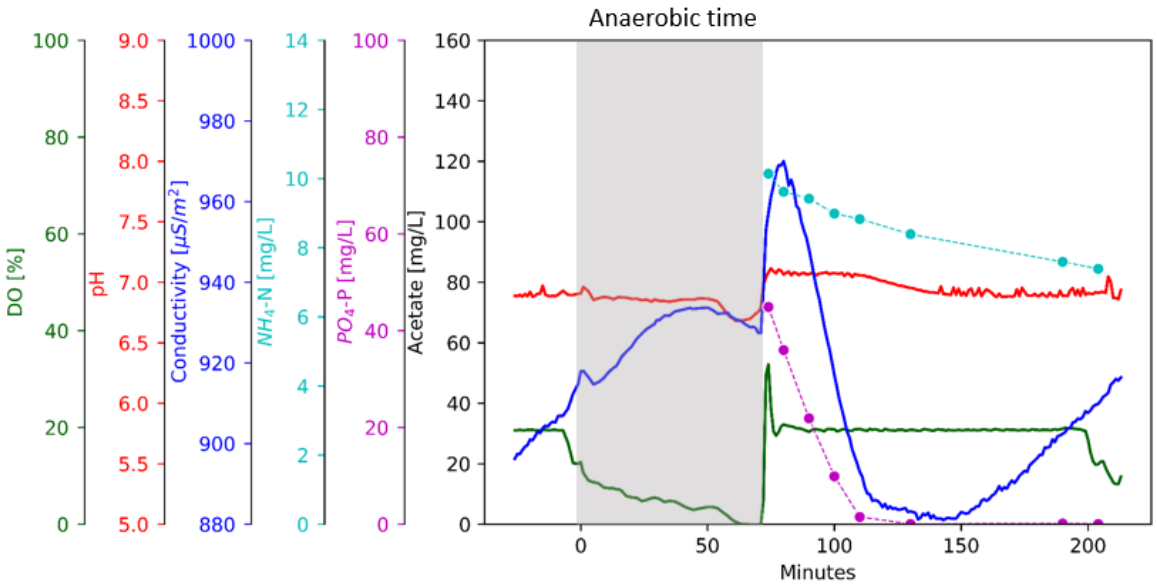

Figure 9: Representation of the dynamics in the bed fed reactor during a cycle

The average reactor properties were obtained via the cycle measurement and reactor operations. These characteristics are shown in Table 2 and are used to compare the behaviour of the lab reactors.

Table 2: Reactor properties after 20 weeks of reactor operations

Steady state values	Pulse fed reactor	Bed fed reactor	Units
Reactor sludge	4.11	4.02	gVSS/L
VSS/TSS	0.77	0.81	gVSS/gTSS
Average Yield	0.33	0.25	gVSS/gCOD
Average Density	31	27	gVSS/Lgranule
SRT	26	21	days
Effluent VSS	0.04	0.02	gVSS/L
Reactor Volume	3	3	L
Effluent Volume	1.4	1.4	L
Acetate uptake rate	2.27	N/A	mg/gVSS/min
PO_4-P release rate	0.93	N/A	mg/gVSS/min
PO_4-P uptake rate	0.61	0.37	mg/gVSS/min
NH_4-N uptake rate	0.80	0.67	mg/gVSS/min
P/COD	0.57	0.32	mgP/mgCOD
N/COD	0.005	0.006	mgN/mgCOD

3.3. Microbial population

FISH staining was performed on the granulated biomass in order to determine the organism dominating the lab-scale reactor. In Figure 10 the FISH staining are shown, the biomass was stained for PAO and GAO, as shown in the top picture. The staining shows that both reactors are dominated by PAO.

Another staining was performed to determine if the PAO strain differed between the reactors. This staining is shown in the bottom picture, indicating that both reactors consist mainly of PAO I.

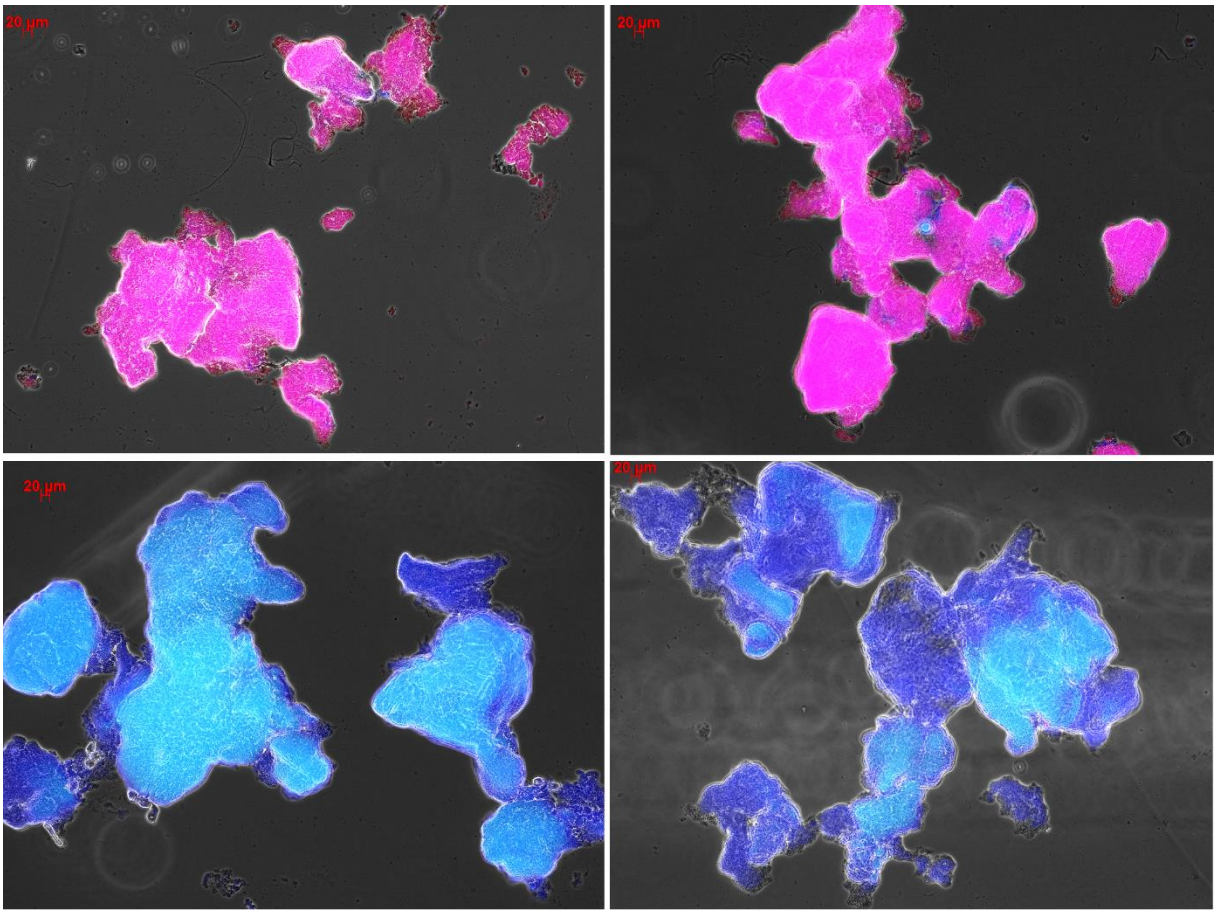

Figure 10: Granules stained with FISH probes from the pulse fed reactor (left) and the bed fed reactor (right). Top pictures are stained for PAO, Eubacteria, GAO (r, b, g). Bottom pictures are stained for ACC2, Eubacteria, ACC1 (r, b, g)

3.4. Density of granules

The absolute biomass density of the granule fractions is shown below. This shows that the average granule density in the pulse fed reactor is almost equal over the fractions, whereas the bed fed reactor has an increasing density over the granule sizes. However, the overall density is lower for the granules in the bed fed reactor than for the pulse fed reactor. This can be caused by the reactor conditions, as the granules in the pulse fed reactor experience higher shear due to the anaerobic mixing. The granules of the full scale installation have a constant density for the granules bigger than 1mm diameter, with an average density comparable to the density of the bed reactor.

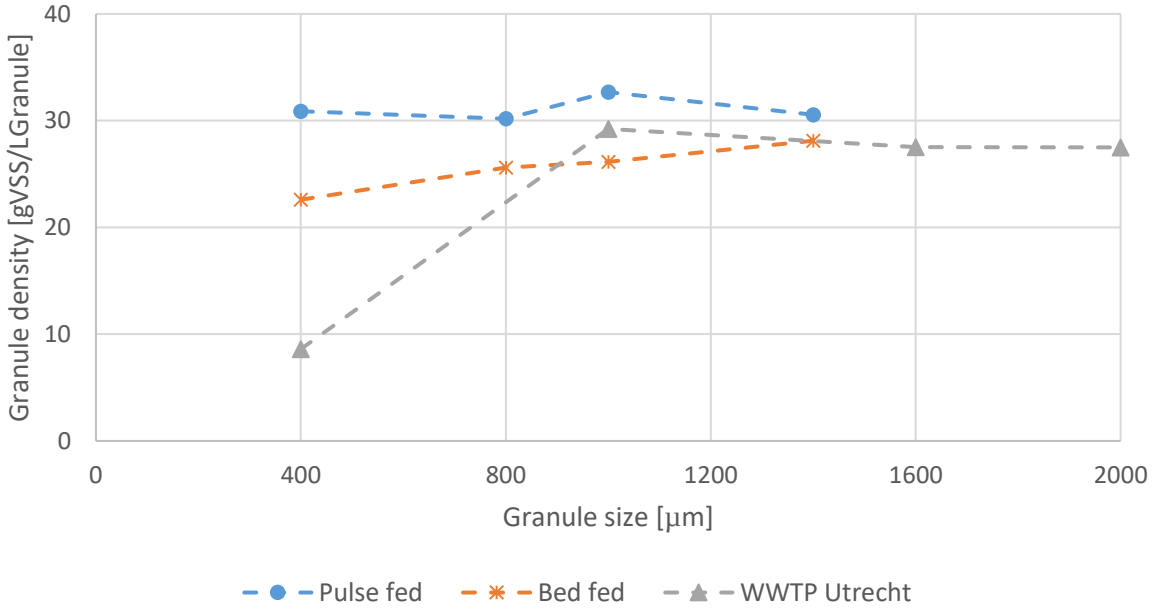

3.5. Granule distribution

The granule distribution in the reactors was determined via image analysis, after having applied an SRT control of on average 20 days for 20 weeks. At this time, more than 65% of the sludge in the pulse fed reactor were granules with a diameter greater than 1mm. In the bed fed reactor, this was more than 80% of the sludge. As less than 1% of the sludge in both reactors was smaller than 400µm diameter, the reactors are considered to be fully granulated.

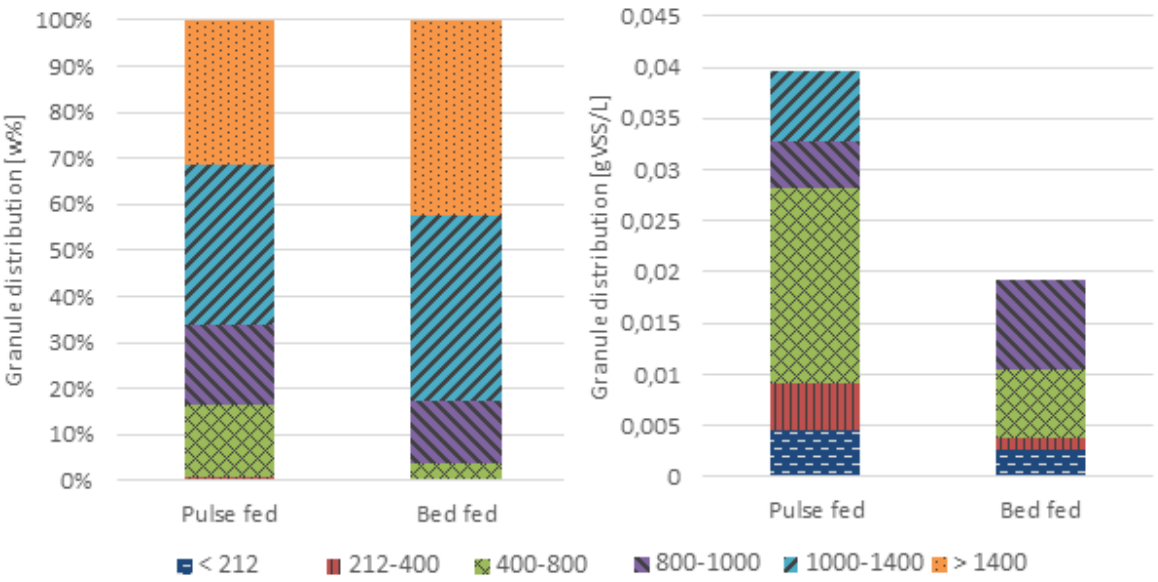

Figure 11: Granular distribution of the pulse fed and bed fed reactor (left) and the weight distribution of the reactor effluent (right)

The effluent granule distribution shows that only granules smaller than 1 mm diameter are removed from the bed fed reactor when applying selective sludge removal based on settling speed. In the effluent of the pulse reactor some bigger granules were found. This is most likely due to deposited granules in the effluent tube during the flush and mixing phases. In general the granules smaller than 400µm diameter are washed out of the reactor as soon as they form.

The combination of granule distribution in the reactor and the known effluent distribution was used to determine the SRT in the lab reactors. Although the average SRT was kept at 20 days in both reactors, the unequal effluent composition and sludge removal via the sample port resulted in a distribution in SRT over the granules. This SRT distribution of the granule fractions at the end of reactor operations is visualised by the blue (●) line in Figure 12. The trend shows that in both reactors the granules bigger than 1mm diameter have an SRT longer than 20 days. As this fraction is not removed via the effluent, and is only limited removed via the manual SRT control. The orange (□) line shows the SRT of the granule fractions when no manual SRT control would be applied. In the pulse fed reactor this would lead to a high SRT for all fractions bigger than 800µm, with an unlimited SRT for the granules bigger than 1400µm. In the bed fed reactor all granules bigger than 1000µm have an unlimited SRT, as these granules were not present in the reactor.

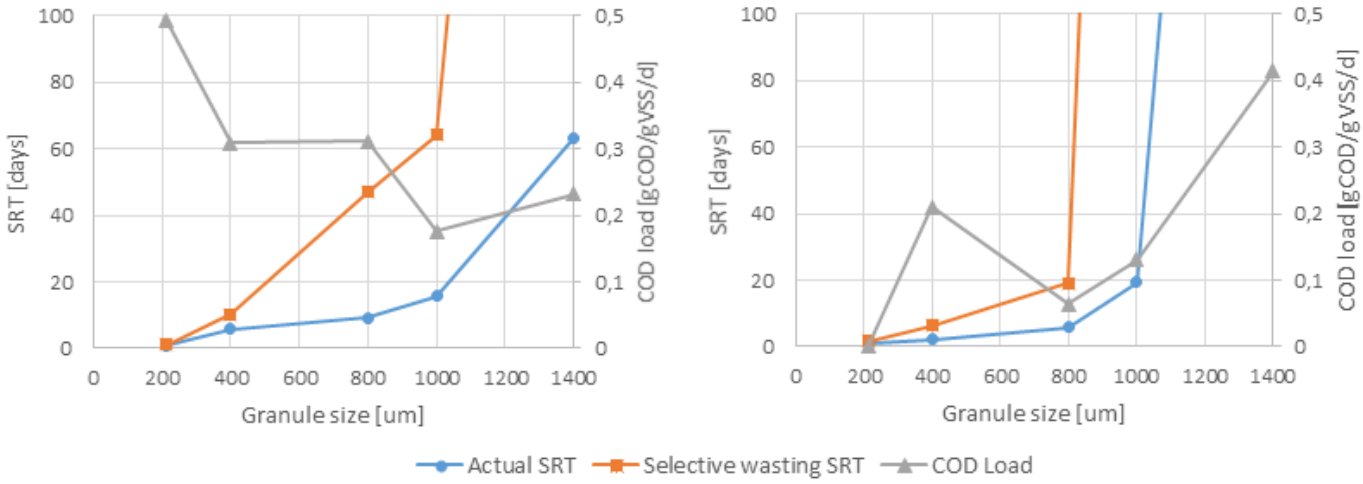

Figure 12: Actual SRT, SRT without manual control and the COD load of the granule fractions of the pulse fed reactor (left) and bed fed reactor (right)

The COD load of the granule fractions is also shown in Figure 12 for the lab reactors. This load is determined by combining the COD distribution and the granule distribution in the reactor. The COD load of the granule fractions in the pulse reactor decreases over the increase of granule size, as the COD distribution is only determined by the diffusion and uptake rates. This favours the smaller granules as they have a bigger surface area per particle volume. In the bed reactor, due to the slow feeding through the bottom, bigger granules are favoured because of their faster settling speed. The 400µm fraction in the bed fed reactor receives some COD, but this data point is uncertain as only 3w% of the reactor biomass is in this fraction. The difference in COD load is determined via the influent contact regime.

3.6. COD distribution over fractions

The PHA content per gram of biomass was measured for the granules of each size, of the pulse fed and bed fed reactor. The difference between the PHA content at the end of the aeration and the PHA content at the end of the anaerobic phase was calculated. The PHA content of the granules are shown in Figure 13. It is notable that in the pulse fed reactor all PHA in the granules is depleted, while the bed fed reactor has a PHA reserve for every granule size at the end of the cycle. The PHA reserve of the granule fractions can be caused by insufficient aeration, resulting in PHA build-up over time.

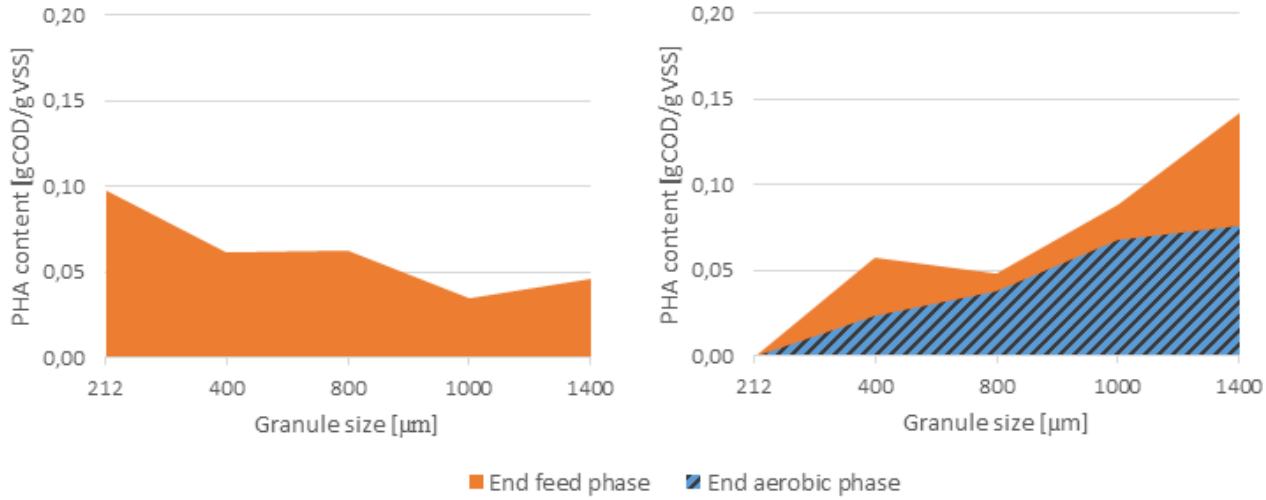

Figure 13: PHA content of granule fractions after influent feeding and at the end of the aerobic phase, of the pulse fed reactor (left) and bed fed reactor (right)

The COD from the influent is divided over the granules depending on the anaerobic contact time and the COD concentration profile. Figure 14 shows the COD distribution over the granule fractions in the reactors in the bed feed reactor, most COD is taken up by the biggest granules (72%) as is expected by the way of influent feeding. In the pulse fed reactor, the COD is more evenly divided over the fractions, with a slight increase over the fractions. Even though the COD load of the bigger granules is lower than the load of the small granules, the total amount of COD is higher due to the granule distribution in the reactor.

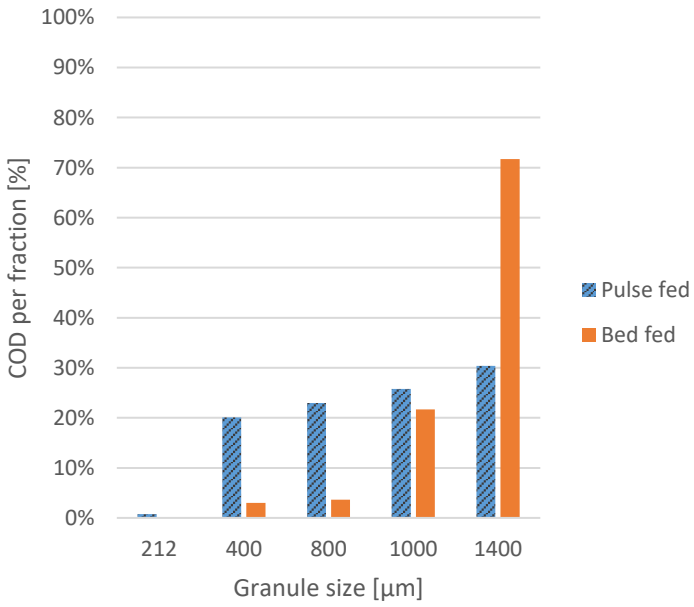

Figure 14: COD distribution of the pulse fed and bed fed reactor

The rates and capacity of the granule fractions can also be used to determine the COD distribution over the reactor. In Figure 15, the COD distribution via the PHA data and the expected COD uptake according to the rates and maximal capacity of the granule fractions is shown. Both graphs show an increasing uptake capacity with increasing granule size. The expected uptake is close to the measured COD uptake in the pulse reactor, showing that the rates determine the COD distribution in this reactor. The expected COD distribution is not equal to the measured COD uptake in the bed fed reactor. In this reactor the granules bigger than1400µm diameter are able to consume 100% of the COD, but the PHA measurements shows these granules consume 72% of the COD. This would indicate incomplete stratification in the bed fed reactor, or dispersion in the plug flow through the sludge bed.

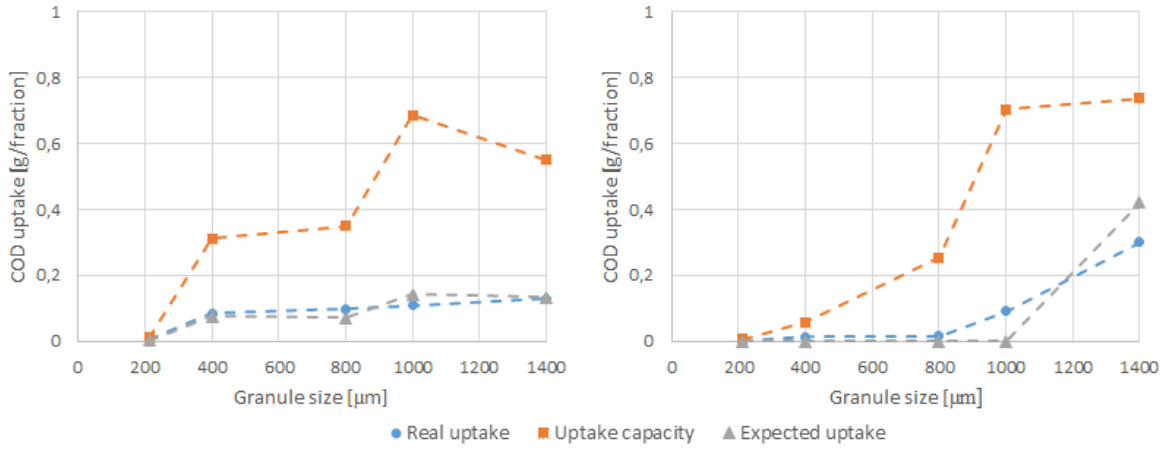

Figure 15: Measured and expected COD uptake and capacity per granule size of the lab scale reactors. Pulse fed reactor (left) and Bed fed reactor (right)

3.7. Granule metabolism

Via the batch test the acetate uptake rate, acetate capacity, phosphate release rate and phosphate capacity per granule fraction were determined. During the batch test, a high acetate concentration was added to the granules to ensure that even big granules are fully penetrated. Differences in rates can only be caused by inactive biomass in the granules, or the presence of different species.

The rates and capacities show a downward trend in the pulse fed reactor. This would indicate a lower biomass activity for the bigger granules. As expected, this would indicate that granules are not completely penetrated in the pulse fed reactor, due to diffusion limitation. Only the outside layer of the granule is actively growing, while the inside of the granules is mainly performing endogenous respiration. The decrease in phosphate rates and capacity would indicate a P-limited metabolism in the centre of the granules.

In the bed fed reactor, the acetate uptake rates and acetate capacity are equal over the granule sizes, with a decrease in phosphate release and capacity for the biggest granules. Acetate values are comparable to the pulse fed reactor. The downward trend in phosphate release was unexpected, as the bigger granules receive a higher COD load during reactor operations. This could indicate a P-limited metabolism in the centre of the granules.

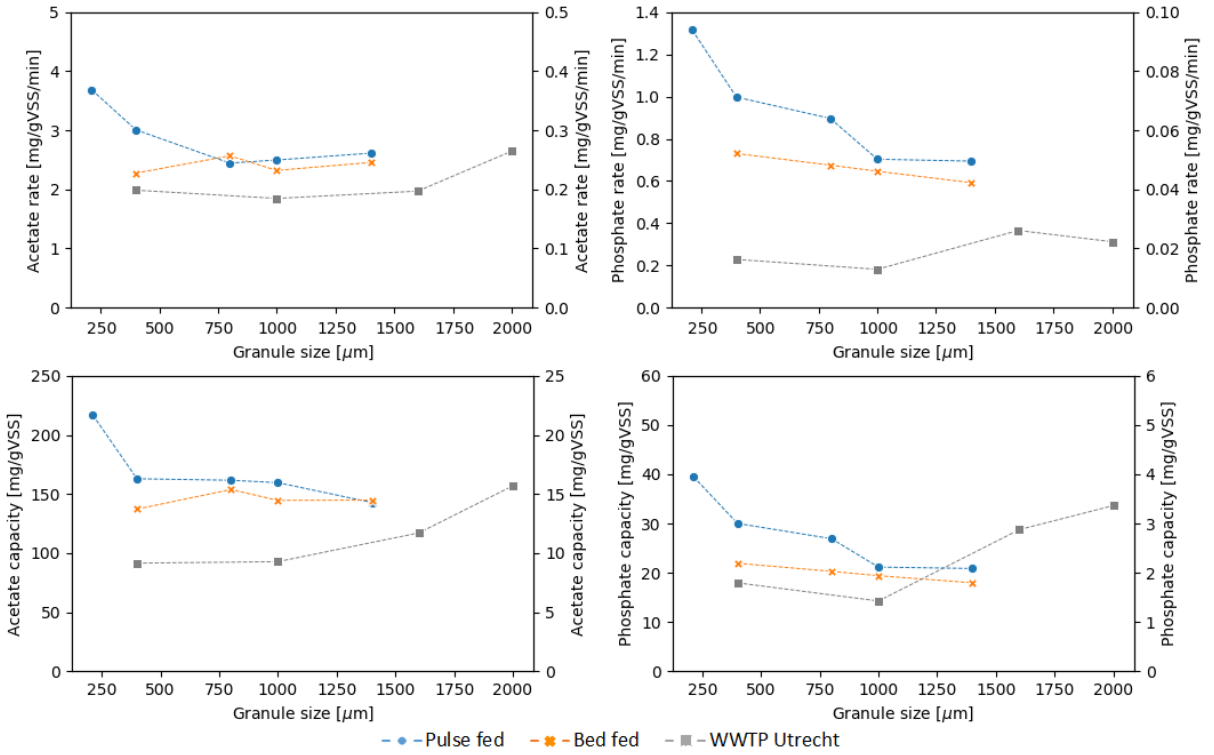

Figure 16: The acetate uptake rates (top left), phosphate release rates (top right), acetate uptake capacity (bottom left), and phosphate release capacity (bottom right). The pulse fed and bed fed reactor are shown on the left axis, the data from WWTP Utrecht is shown on the right axis

The full scale granules from WWTP Utrecht showed an opposite trend to the lab-scale reactors, with an increase in rate and capacity over granule size. The observed rates and capacity are 10x lower than the lab-scale rates. An increasing line over granule size can only be explained by a shift in PAO abundance over the granule sizes in full-scale Nereda™.

The P/COD gives the ratio of mg phosphate released per mg acetate uptake of the granule. This rate can indicate a shift of metabolism of the PAO in the granules. The expected P/COD rate for PAO at an SRT of 20 days is 0.5-0.6 mgP/mgCOD at pH 7 (Smolders *et al.*, 1996) The P/COD ratio in the cycle measurement is 0.57 mgP/mgCOD in the pulse fed reactor, and 0.32 mgP/mgCOD in the bed fed reactor. The ratio in the pulse reactor at the moment of COD depletion is 0.41 mgP/mgCOD. In Figure 17 the P/COD ratio in mgP/mgCOD from the batch tests is shown. The bed fed reactor shows a decrease in P/COD ratio for bigger granule sizes. On average the P/COD ratio was 0.24 mgP/mgCOD for the pulse fed reactor, and 0.23 mgP/mgCOD in the bed fed reactor. The P/COD ratio in the pulse fed reactor does not differ more than 0.02 mgP/mgCOD from the average. Therefore the P/COD ratio does not change in the pulse fed reactor over the granule sizes. In a full-scale Nereda™ plant the big granules show a higher P/COD than the smaller granules.

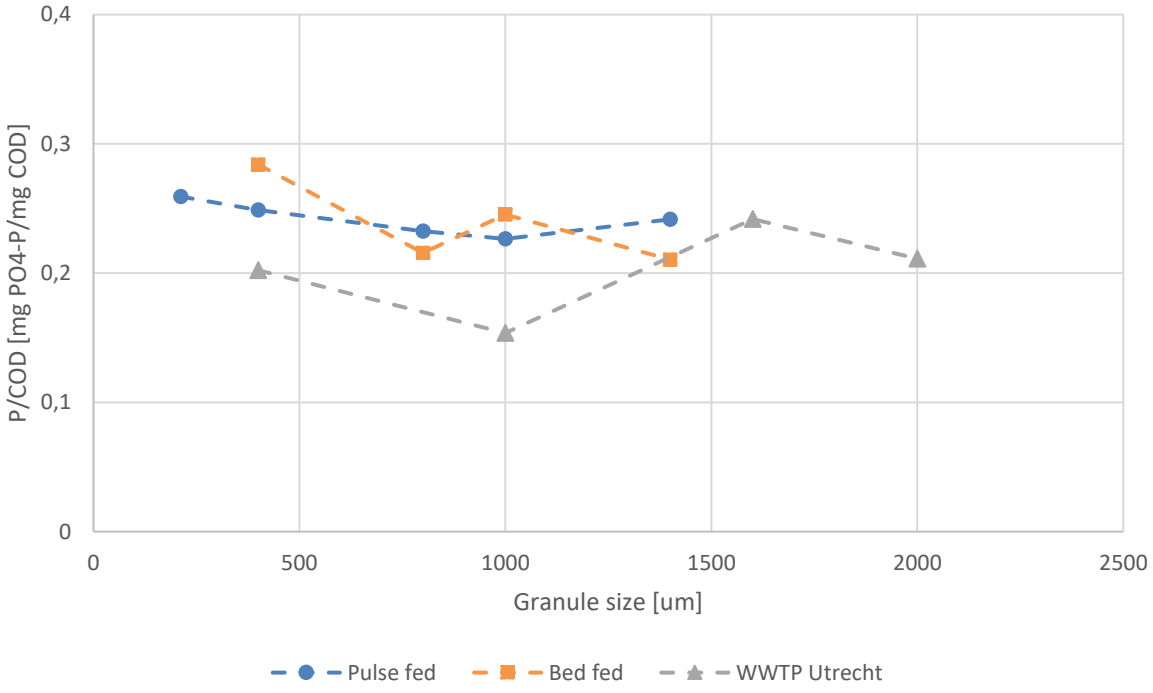

Figure 17: P/COD ratio of the pulse fed and bed fed reactor, and granules from WWTP Utrecht

3.8. Reactor dynamics

Biomass shift between the bins in the dynamic steady state can be determined, by setting up a mass balance over the granule fractions. The biomass shifts are the difference of biomass growth in the fraction by the received COD and the removal of granules from the fraction via the selective effluent and SRT control. This biomass shift is the sum of the net biomass growth and detachment from the granules.

Figure 18 and Figure 19 show the COD distribution, relative mass of the granules fractions and VSS removal of the granule size fractions in the pulse fed and bed fed reactor. The green arrow indicates the biomass change of the granule fraction, this amount was calculated by assuming the biomass change in a granule fraction is equal to zero in the dynamic steady state.

The difference between the reactors is due to the anaerobic contact regime. In the bed fed reactor bigger granules receive a higher COD load, compared to the pulse fed reactor. 94% of the COD is consumed by granules bigger than 1mm diameter in size, while the COD in the pulse fed reactor is more evenly spread over the fractions, with 56% of the COD consumed by granules bigger than 1mm diameter.

Both models show the same sludge removal trend, where the small granules are mainly removed via the effluent, and the bigger granules are only removed via the SRT control. Even with the SRT control, only a small fraction of the big granules leave the lab-scale reactors, due to suboptimal sludge removal.

In both reactors the sum of growth and decay for the granules bigger than 1400μm diameter, gives a net flow of biomass leaving the fraction, indicated by the green arrow. This biomass could be growth to a bigger fraction, or detachment of biomass towards a smaller granule fraction. The granule fractions 1000μm and 800μm in the pulse fed reactor show a negligible biomass change in the fraction, meaning that the sum of granule decay and granule growth equals out. In the bed fed reactor, only the 1000μm fraction has a negligible biomass flow. The small granule fractions do not receive enough COD to sustain their presence in the reactor, as this fraction is removed daily from the reactor, mostly via the effluent. This makes it likely that e.g. shear from the big granules contributes to the presence of the small granules. The combination of selective biomass removal and influent contact regime show a high pressure towards granules bigger than 1000μm in the bed fed reactor compared to the pulse fed reactor.

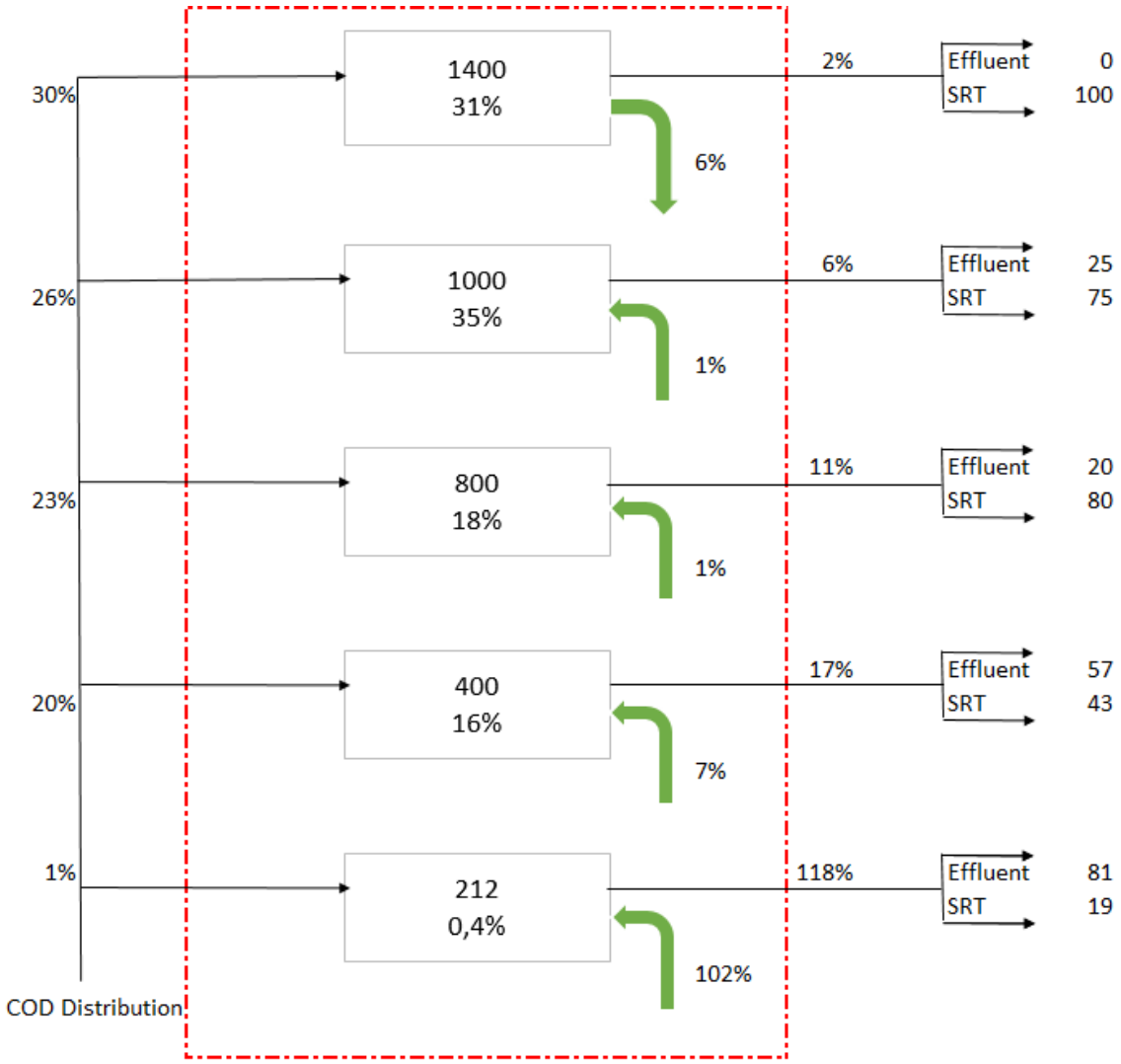

Figure 18: Mass balance of the pulse fed reactor. The left arrows show the COD distribution of the influent over the granule sizes in w%. The granule fractions show the w% of the granule size in the reactor after 140 operation days. The black arrows leaving the reactor is the w% of the granules leaving that fraction per day on average. This removal is the sum of removal via the selective settling pressure and the manual SRT control, the distribution between these removal methods is in w%. The green arrows leaving or entering a fraction show the w% of biomass change in the fraction per day. The biomass change is the sum of i.a. growth, detachment and attachment.

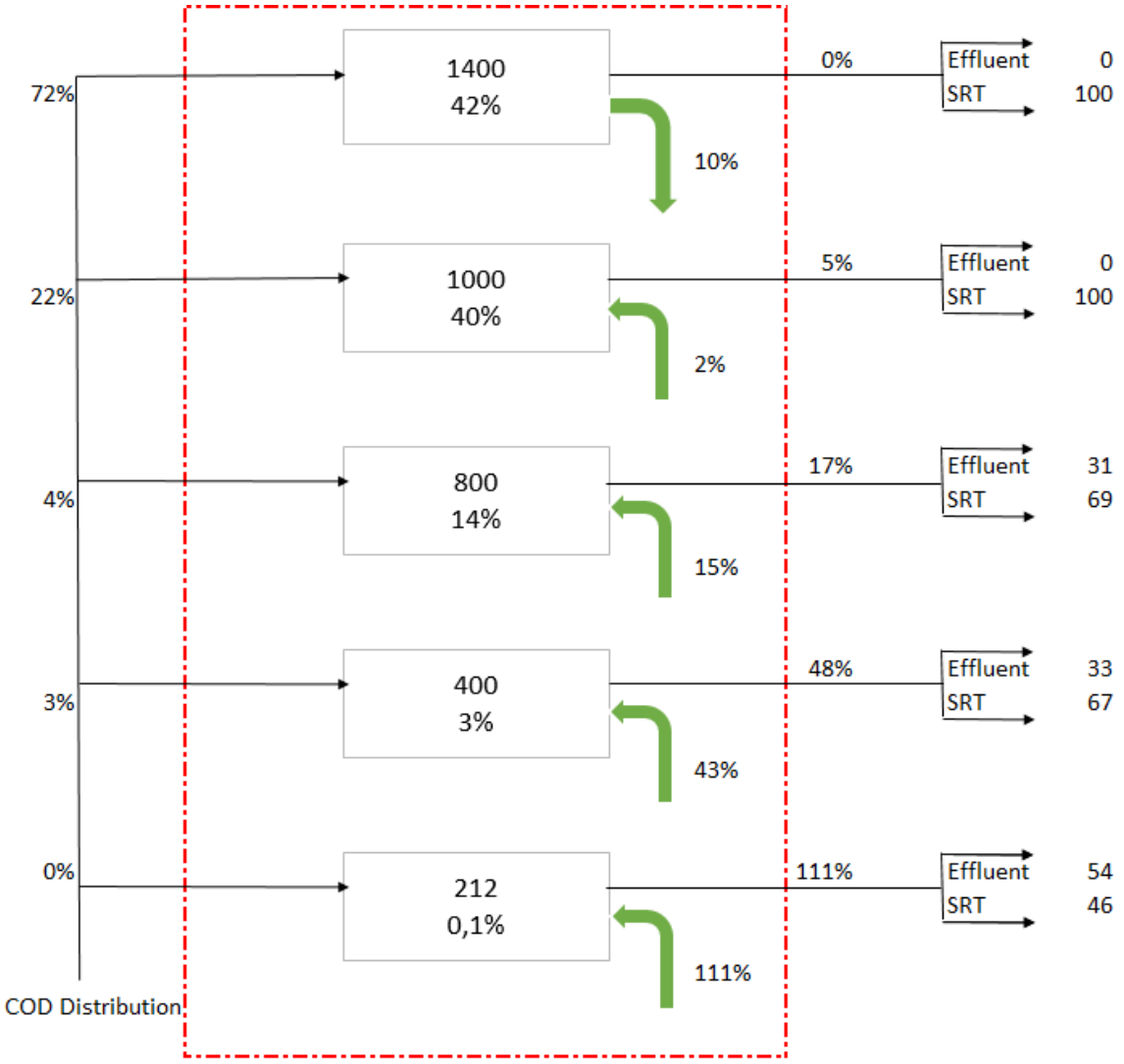

Figure 19: Mass balance of the bed fed reactor. The left arrows show the COD distribution of the influent over the granule sizes in w%. The granule fractions show the w% of the granule size in the reactor after 140 operation days. The black arrows leaving the reactor is the w% of the granules leaving that fraction per day on average. This removal is the sum of removal via the selective settling pressure and the manual SRT control, the distribution between these removal methods is in w%. The green arrows leaving or entering a fraction show the w% of biomass change in the fraction per day. The biomass change is the sum of i.a. growth, shear, detachment and attachment.

4. Discussion

4.1. Start-up reactors and granulation speed

The pulse fed reactor was easier to start-up to get initial granules. As the bed fed reactor was initially anaerobically overloaded due to formation of preferential flow-channels during the anaerobic contact phase. The required plug-flow for the bed fed reactor is not easily established without a granulated sludge bed. For lab-scale reactors, it could be beneficial to start-up with a pulse system, and then switch to bed feed when a granulation is established.

The maximum growth speed of the granules was determined via tracking the first significant occurrence of a granule size in the lab-scale reactors. This resulted in a growth speed of 26µm/day in the pulse fed reactor, and a growth speed of 40µm/day in the bed fed reactor. The faster growth speed of the bed fed reactor was expected, as the influent regime results in a higher COD load, and thus growth for granules on the bottom of the reactor.

As a difference in reactor composition at the end of the experiment, when using a different sample method, compared to the previous distribution was found. A sampling error seems to result in an underestimation of the granules bigger than 1000µm diameter. This is most likely due to suboptimal mixing by aeration. However, the data shows that it is possible to characterise the granule size and growth of a reactor with image analysis.

4.2. Reactor operations

From the combination of the online data and the offline PO_4-P data, it is shown that the conductivity trends can be used to track phosphate release and uptake of the granular sludge in the pulse fed reactor. It was observed that phosphate release continues in the pulse reactor even when acetate was depleted. The PO_4-P concentration increase between 15 and 30 minutes is notable, as this trend is not generally observed. In other research the PO_4-P concentration is stable after COD depletion, with a slight increase from endogenous phosphate release (Acevedo *et al.*, 2012; Welles *et al.*, 2015). The endogenous phosphate release is seen between 30 and 60 minutes, with a rate of 0.02 mgP/gVSS/min. The phosphate release after acetate depletion could be due to diffusion from inside the granule to the bulk liquid.

As ATU is added to the reactor, NH_4 is only consumed for growth. The NH_4-N trend shows that during the aeration time, granular growth takes place. The bed fed reactor shows a continuous decrease of NH_4-N until the aeration is stopped. This indicates that the sludge is still growing at the end of the cycle. This would be likely as the PHA data shows that there are still storage polymers available in the granules, in contrary to the pulse fed reactor. This could be due to slow diffusion of oxygen into the granules and thus limiting growth. Growth limitation due to oxygen deficiency in the granule centre is likely, as the yield and NH_4-H consumption rate are lower in the bed fed reactor. In the pulse fed reactor a constant NH_4-N concentration is seen at the end of the aeration, indicating the depletion of storage polymers.

4.3. Granule size and COD distribution

After 140 days of reactor operations, both reactors were fully granulated. More than 65 w% of the sludge in the pulse fed reactor consist of granules bigger than 1 mm diameter. For the bed reactor, this was more than 80w% of the sludge. The COD-distribution in the reactors led to a dynamic steady state, with movement of the biomass over the different fractions.

The COD in the pulse fed reactor was divided over the granule fractions based on uptake rate and mass fractions in the reactor. This combination led to an almost equal COD-distribution over the fractions, even though the bigger granules had a slower acetate uptake rate than the small granules. This can also be deduced from the lower COD-load of the bigger granule size fractions. The decreasing rates and the capacities with respect to granule size was found in the pulse fed reactor. This can be explained by a low COD concentration in the centre of the granule, due to the sum of acetate uptake and diffusion. Penetration depth calculations according to Pérez *et al*. (2005) show that at the start of the anaerobic phase, the whole granule is penetrated with COD. However, in the centre of the granule, this COD concentration is lower than the concentration at the outer layers of the granule. This would suggest an activity gradient over the depth of the granule, where biomass in the centre of the granule is mainly performing endogenous respiration, while the biomass in the outer layer is growing. In the bed reactor, big granules receive a higher COD load than the small granules, due to the influent regime. This is clearly visible by the COD-load and the COD-distribution. 72% of the influent COD is consumed by the granules fraction bigger than 1400µm diameter. According to the acetate uptake capacity and uptake rate, in combination with the up flow speed through the bed, 100% of the COD should be consumed by the granule fraction bigger than 1400µm. As there is still COD consumption by the other granules, incomplete stratification and dispersion over the sludge bed are most likely present during the feeding phase.

The COD distribution determines the possible growth of a fraction, therefore the anaerobic influent contact regime greatly influences the granule distribution of a reactor.

4.4. Granule stoichiometry

By comparing the P/COD ratio of the pulse fed and bed fed reactor with the P/COD ratios found via the batch tests, shifts in metabolism can be found with respect to the granule sizes. These shifts can indicate the presence of diffusion limitation during reactor operations.

The P/COD ratio in the bed fed reactor during the cycle measurement is 0.32 mgP/mgCOD. It is not possible to exert pH control on the bed fed reactor during the feeding phase, due to the plug flow feeding through the bed. The pH during the feed is therefore equal to the medium pH, which is 6. The P/COD ratio at this pH is 0.3 mgP/mgCOD (Smolders *et al.*, 1994), so this value is as expected. During the batch test, the P/COD ratio is lower, 0.23 mgP/mgCOD on average. Even though the pH was set at 7, and buffered with a HEPES buffer during the batchtest, so more P release would be expected to take up the acetate. The low P/COD could indicate a pH gradient in the granules, where the pH in the granules is still close to 6, or a shift to a P-limited metabolism compared to the stoichiometry in the reactor. This could explain the lower P/COD ratio of the granules bigger than 1400µm, as COD is present over the whole depth of the granule, while the diffusion of phosphate into the granule could be slower than the phosphate uptake rate.

The P/COD ratio in the pulse reactor during the normal cycle was 0.57 mgP/mgCOD. (Smolders *et al.*, 1994) shows that the P/COD ratio for PAO at an SRT of 20 days is 0.5-0.6 mgP/mgCOD at pH 7, therefore, the found value is according to expectations. During the batch test, an average P/COD ratio of 0.3 mgP/mgCOD was found. This could indicate a more P-limited metabolism in the batch test than in the reactor. It is possible that over the depth of the granule a shift in metabolism takes place, where the outside layer uses phosphate to fuel acetate uptake, and the inside of the granule operates under more phosphate limiting conditions.

4.5. Density

The density of the pulse fed reactor was equal for all granule sizes, while the density of granules increased with the size in the bed fed reactor. The granules from the pulse fed reactor had a higher density than the granules of the bed fed reactor. Granules from a full scale Nereda™ WWTP are comparable to the bed fed reactor in terms of density. The found density value is significantly lower than the density found by (De Kreuk *et al.*, 2005). In this research a density of 78 g VSS/L biomass was reported. The density in the pulse reactor is likely higher due to higher average shear in the reactor because of anaerobic mixing using nitrogen gas.

4.6. Full-scale behaviour

The full-scale granules show a different behaviour than the lab-scale granules. In the full-scale an increase in acetate uptake rate, acetate uptake capacity, phosphate release rate and phosphate release capacity were observed with increasing granule size. However, the rates for all size fractions were ten times lower than the rates and capacity in the lab scale reactors. Insufficient aeration could have resulted in incomplete PHA degradation prior to the performing the anaerobic batch test. Data obtained for the different granule size fractions in the full-scale sludge sample from Utrecht WWTP can however still be compared. At the high acetate concentration in the batch tests, an increase with respect to granule size can be attributed to several reasons. An increased enrichment for anaerobic storage metabolism with increasing granule size would support such a trend.

This difference in microbial population was most likely caused by the presence of different COD sources in wastewater. The available VFAs are taken up by the granules at the bottom of the reactor due to the plug flow feeding through the bed, leaving other particulate COD for the smaller granules. This COD has either first to be hydrolysed and fermented prior to anaerobic storage, or can only be oxidized aerobically.

4.7. Effect of granule population dynamics and anaerobic contact regime on biomass

The biomass removal, granular growth, and granule distribution are combined in the mass balance over the granule fractions. The influence of the selective settling pressure is visible by the shift of biomass removal mainly via the effluent, to a removal mainly via the SRT control for the fractions with increasing granule size. Furthermore, the biomass shifts between fractions within the reactor due to detachment of fragments from larger granules to smaller granule fractions and growth of new biomass on the surface of these granules. The net result of the aforementioned mechanisms was that the granule SRT is not necessarily equal to the biomass SRT.

The COD load increased over the granule size in the bed reactor, due to the plug flow though the bed. This resulted in a high COD load for the granules bigger than 1400µm in diameter. During reactor operations with the aim of nutrient removal, phosphorous removal and processes as SND would occur in this fraction. However, biological phosphorus removal works on the principal of removal through stored phosphate in biomass through sludge wasting. The combination of high COD load and long SRT can result into problems with phosphate removal in these reactors. As phosphate is not removed from the system via biomass wasting, a build-up of phosphate occurs in the granules. When growth of these granules is limited by insufficient aeration, phosphate uptake capacity may decrease, as this is limited to growth.

In the pulse fed reactor, a lower COD load is observed over the granules with high SRT and no growth limitation was observed. However the spatial COD limitation over the depth of the granule could prevent the occurrence of processes as SND in a full-scale reactor.

Therefore the anaerobic contact regime also has an effect on the biological conversions required for biological nutrient removal, especially biological phosphorus removal. Determination of the phosphorus content of the biomass in the granule size fractions could give more insight on this relation.

5. Conclusions

- ✓ During start-up the granular growth rate is faster in the bed fed reactor compared to the pulse fed reactor, when looking at the first occurrence of granules of a certain size. The maximal growth speed is 26 μm/day for granules in the pulse fed reactor and 40 μm/day in the bed fed reactor.

- ✓ Growth distribution during the dynamic steady state resulted a higher mass fraction of granules greater than 1mm diameter in the bed fed reactor.
  - ➢ In the pulse fed reactor growth is almost equally divided over all fractions, because of the interplay of granule size mass fraction and biomass specific uptake rates.
  - ➢ In the dynamic steady state the main growth is located in the granules bigger than 1400μm in the bed fed reactor. Smaller fractions have a short SRT and exist mainly due to detachment.

- ✓ The difference in rates in respect to granule size shows diffusion limitation during normal reactor operations.
  - ➢ The decreasing acetate uptake rate with respect to the granule size suggest diffusion limitation during normal reactor operations in the pulse fed reactor. The equal acetate uptake rate over granule size indicates a shift to GAM in the granules of the bed fed reactor.
  - ➢ The decreasing PO_4-P release rate in both lab-scale reactors, combined with the observed PO_4-P release after COD depletion in the pulse fed reactor, suggests PO_4-P diffusion limitation from the granules to the bulk liquid.
  - ➢ The increasing acetate and PO_4-P rates in the granules from WWTP Utrecht indicates a microbial shift over the granule sizes.

- ✓ Due to the difference in anaerobic contact regime the biomass loading rate decreases for increasing granule size in the pulse fed reactor, while it increases in the bed fed reactor.
  This leads to a higher spatial COD load distribution in the largest granule fraction in the pulse fed reactor than the bed fed reactor.

- ✓ The difference in P/COD ratio between the batch tests and the cycle measurements indicate P-limited conditions.
  - ➢ The P/COD ratio in the pulse fed reactor is not comparable to the P/COD ratios of the batch tests. The lower P release would indicate a difference in poly-P content over the depth of the granules.
  - ➢ The P/COD ratios in the bed fed reactor are not the same for the batch tests and cycle measurement, but the difference is not as great as in the pulse fed reactor. The combination of pH and poly-P availability in the granules can explain the lower P/COD ratios in the bed fed reactor.

- ✓ The average granule density is higher in the pulse fed reactor than the average granule density of the bed fed reactor. The density of the granules from WWTP Utrecht are comparable to the density of the lab-scale reactors. The found density significantly lower than the commonly used granule density in AGS models.

6. Outlook

- The difference in P/COD ratio for the same granule size depending on anaerobic contact regime, warrants further investigation of the phosphate distribution within the granule. Since this is likely of importance for the stability of full scale phosphorus removal.
- Incorporate recent insights in the metabolic response of PAO under P-limiting conditions (Welles *et al.*, 2015) and dependence on pH into a biofilm model to investigate the effect of anaerobic contact regime on the performance of biological phosphorous removal.

References

ACEVEDO, B. et al. Metabolic shift of polyphosphate-accumulating organisms with different levels of polyphosphate storage. **Water Research,** v. 46, n. 6, p. 1889-1900, 2012/04/15/ 2012. ISSN 0043-1354. Available at: < http://www.sciencedirect.com/science/article/pii/S0043135412000097 >.

AMANATIDOU, E. et al. Influence of wastewater treatment plants' operational conditions on activated sludge microbiological and morphological characteristics. **Environmental Technology,** v. 37, n. 2, p. 265-278, 2016/01/17 2016. ISSN 0959-3330. Available at: < https://doi.org/10.1080/09593330.2015.1068379 >.

BEUN, J. J.; VAN LOOSDRECHT, M. C. M.; HEIJNEN, J. J. Aerobic granulation in a sequencing batch airlift reactor. **Water Research,** v. 36, n. 3, p. 702-712, 2002/02/01/ 2002. ISSN 0043-1354. Available at: < http://www.sciencedirect.com/science/article/pii/S0043135401002500 >.

DE KREUK, M.; VAN LOOSDRECHT, M. Selection of Slow Growing Organisms as a Means for Aerobic Granular Sludge Stability. **Water science and technology : a journal of the International Association on Water Pollution Research,** v. 49, p. 9-17, 02/01 2004.

DE KREUK, M. K.; HEIJNEN, J. J.; VAN LOOSDRECHT, M. C. M. Simultaneous COD, nitrogen, and phosphate removal by aerobic granular sludge. v. 90, n. 6, p. 761-769, 2005. ISSN 0006-3592. Available at: < https://onlinelibrary.wiley.com/doi/abs/10.1002/bit.20470 >.

JAFARINEJAD, S. J. A. W. S. Cost estimation and economical evaluation of three configurations of activated sludge process for a wastewater treatment plant (WWTP) using simulation. v. 7, n. 5, p. 2513-2521, September 01 2017. ISSN 2190-5495. Available at: < https://doi.org/10.1007/s13201-016-0446-8 >.

JOHNSON, K. et al. Enrichment of a Mixed Bacterial Culture with a High Polyhydroxyalkanoate Storage Capacity. **Biomacromolecules,** v. 10, n. 4, p. 670-676, 2009/04/13 2009. ISSN 1525-7797. Available at: < https://doi.org/10.1021/bm8013796 >.

KENT, T. R.; BOTT, C. B.; WANG, Z.-W. State of the art of aerobic granulation in continuous flow bioreactors. **Biotechnology Advances,** v. 36, n. 4, p. 1139-1166, 2018/07/01/ 2018. ISSN 0734-9750. Available at: < http://www.sciencedirect.com/science/article/pii/S0734975018300661 >.

MOSQUERA-CORRAL, A. et al. Effects of oxygen concentration on N-removal in an aerobic granular sludge reactor. **Water Research,** v. 39, n. 12, p. 2676-2686, 2005/07/01/ 2005. ISSN 0043-1354. Available at: < http://www.sciencedirect.com/science/article/pii/S0043135405002356 >.

PICIOREANU, C.; LOOSDRECHT, M. C. M. V.; HEIJNEN, J. J. Discrete-differential modelling of biofilm structure. **Water Science and Technology,** v. 39, n. 7, p. 115-122, 1999/01/01/ 1999. ISSN 0273-1223. Available at: < http://www.sciencedirect.com/science/article/pii/S0273122399001584 >.

PRONK, M. et al. Full scale performance of the aerobic granular sludge process for sewage treatment. **Water Research,** v. 84, p. 207-217, 2015/11/01/ 2015. ISSN 0043-1354. Available at: < http://www.sciencedirect.com/science/article/pii/S0043135415301147 >.

SMOLDERS, G. J. F. et al. Model of the anaerobic metabolism of the biological phosphorus removal process: Stoichiometry and pH influence. v. 43, n. 6, p. 461-470, 1994. ISSN 0006-3592. Available at: < https://onlinelibrary.wiley.com/doi/abs/10.1002/bit.260430605 >.

SMOLDERS, G. J. F.; VAN LOOSDRECHT, M. C. M.; HEIJNEN, J. J. Steady-state analysis to evaluate the phosphate removal capacity and acetate requirement of biological phosphorus removing mainstream and sidestream process configurations. **Water Research,** v. 30, n. 11, p. 2748-2760, 1996/11/01/ 1996. ISSN 0043-1354. Available at: < http://www.sciencedirect.com/science/article/pii/S0043135496001273 >.

WELLES, L. et al. Accumulibacter clades Type I and II performing kinetically different glycogen-accumulating organisms metabolisms for anaerobic substrate uptake. **Water Research,** v. 83, p. 354-366, 2015/10/15/ 2015. ISSN 0043-1354. Available at: < http://www.sciencedirect.com/science/article/pii/S004313541530097X >.